



Originally published as:

van Berk, W., Fu, Y., Schulz, H.-M. (2015): Temporal and spatial development of scaling in reservoir aquifers triggered by seawater injection: Three-dimensional reactive mass transport modeling of water-rock-gas interactions. - *Journal of Petroleum Science and Engineering*, 135, p. 206-217.

DOI: <http://doi.org/10.1016/j.petrol.2015.09.014>



ELSEVIER

Contents lists available at ScienceDirect

Journal of Petroleum Science and Engineering

journal homepage: www.elsevier.com/locate/petrol

Temporal and spatial development of scaling in reservoir aquifers triggered by seawater injection: Three-dimensional reactive mass transport modeling of water–rock–gas interactions



Wolfgang van Berk^{a,*}, Yunjiao Fu^b, Hans-Martin Schulz^b

^a Clausthal University of Technology, Department of Hydrogeology, Leibnizstraße 10, 38678 Clausthal-Zellerfeld, Germany

^b Helmholtz Center Potsdam – GFZ German Research Center for Geosciences, Section 4.3 Organic Geochemistry, Telegrafenberg, D-14473 Potsdam, Germany

ARTICLE INFO

Article history:

Received 5 May 2015

Received in revised form

17 August 2015

Accepted 10 September 2015

Available online 14 September 2015

Keywords:

Scale formation

Formation damage

Seawater injection

Risk assessment

3D mass transport modeling

ABSTRACT

A new numerical modeling approach enables us to calculate the spatial and temporal development of chemical water–rock–gas interactions, including scaling in oil reservoirs which undergo seawater injection. This approach links such simultaneous hydrogeochemical interactions with the three-dimensional flow of pore water in a semi-generic reservoir aquifer.

Zero-dimensional modeling and calculating saturation indices, which are based on just one seawater and one formation water analysis, are commonly used to evaluate the type and the intensity of wellbore scaling. This type of generalization about the fate and behavior of minerals (dissolution or precipitation) is incapable of correctly predicting scale formation. Our modeling results show that scaling and other water–rock–gas interactions are integrated in a complex web and are coupled to the flow of pore water. Even the same mineral shows different hydrogeochemical behaviors at different reservoir locations. In our case study, calcite dissolves near the injectors and is precipitated within the producers. The injection strategy determines hydraulic processes which lead to the mixing of seawater with formation water throughout the reservoir aquifer and within producers. Consequently, non-autoscales newly form (1) widely within the reservoir aquifer due to dispersion, and (2) intensively at the spots where the margins of seawater plumes approach to and converge close to the producers. On the other hand, water injection triggers the dissolution of primary minerals. Consequently, aqueous ions are released into pore water which later flows to producers. Such ions can be sequestered as scale minerals in the reservoir aquifers or in the producers. Thus, coupled hydraulic and hydrogeochemical processes constantly alter the composition of seawater. Accordingly, original seawater will not reach the producer.

In terms of equilibrium thermodynamics, scaling is an inevitable consequence of seawater injection. However, our modeling results reveal that several parameters that could be technically controlled can strongly affect the intensity of scaling processes as well as their spatial and temporal development, for example, the spatial arrangement of injectors and producers, decrease in total pressure, and CO₂ partial pressure in the pressure drop zone surrounding producers.

Our study demonstrates that three-dimensional modeling is a useful tool for identifying the type of scale minerals and for quantifying their spatial and temporal distribution. It can help to predict the areas where the porosity and permeability properties of reservoirs strongly change due to mineral dissolution and/or precipitation induced by seawater injection. Different modeling scenarios can be calculated for case-specific hydrogeochemical and hydraulic conditions in oilfields of interest. The results gained about the distribution, the amount and the timing of scale formation help to optimize the water injection strategy in order to avoid the “worst case” of scale formation in reservoirs to extend the wellbore life.

© 2015 The Authors. Published by Elsevier B.V. This is an open access article under the CC BY-NC-ND license (<http://creativecommons.org/licenses/by-nc-nd/4.0/>).

1. Background

Reservoir aquifer rocks underwent diverse stages of diagenetic

processes and reactions which altered their mineralogical, geochemical and petrophysical properties. The re-mineralization of sedimentary organic matter induces hydrogeochemical processes (e.g., sulfate reduction, methanogenesis) during early diagenesis. Later, changes in temperature and pressure conditions occur during further burial. The resulting mass transport (e.g., advection of fluids bearing gas, water, and oil; diffusion through free pore water

* Corresponding author. Fax: +49 5323 722903.

E-mail address: wolfgang.van.berk@tu-clausthal.de (W. van Berk).

and/or irreducible, connate formation water) establishes “new” diagenetic environments. In consequence, hydrogeochemical re-equilibration is induced as water–rock–gas interactions in reservoir rocks, including (1) dissolution of unstable minerals, (2) precipitation of stable, newly formed mineral phases, (3) dissolution of gases or their outgassing, and (4) compositional changes of the coexisting pore water. At greater depths, oil degradation could be another aspect of this re-equilibration and drives further diagenetic rock alteration (Ehrenberg and Jakobsen, 2001; van Berk et al., 2013). Such reactions caused by oil degradation may have been active over geological timescales.

Compared to long-term geological processes, reservoir aquifer rocks can be more strongly affected by technical measures. Seawater injection into oil reservoirs as one example is one of the most common oil recovery methods applied in offshore reservoirs (Guan et al., 2005; Bader, 2007), and represents a further stage of diagenetic reservoir rock alteration. Most reservoir rocks can be considered to be chemically reactive when exposed to seawater. A series of hydrogeochemical interactions (including scaling) among injected seawater, rock matrix and coexisting gas could quickly reach (near-) equilibrium conditions in reservoir conditions (Houston et al., 2007; Fu et al., 2012). Therefore, specific hydrogeochemical and physicochemical processes evolve as inevitable consequences of chemical equilibrium-thermodynamics. Their effects are widespread, often described, and of economic importance for the oil industry (Crabtree et al., 1999; Kan and Tomson, 2011). During injection, newly formed minerals coat wellbore tubulars and rock surfaces (overview in Kan and Tomson (2011)). Consequently, this causes decreasing wellbore productivity and/or chemical formation damage, which is characterized by a reduction in the permeability of the rock matrix. Scale formation within the reservoir aquifer (including producers) can be divided into three different types:

(1) “Non-autoscale” formation (e.g., barite, celestite, or calcite; depending on the chemical composition of the injected water and formation water) resulting from the mixing of injected seawater and formation water. For example, the admixture of low-sulfate formation water with high barium and strontium concentrations into sulfate-rich seawater causes Sr-barite deposition with intense mass transfer within reservoir rocks and producers. This scaling, often observed, is due to the extremely low solubility of strontium-bearing barite.

(2) “Autoscale” formation within producers due to a drop in pressure and temperature during fluid production (“scale terminology” according to Crabtree et al. (1999); overview in Kan and Tomson (2011)). The solubility of scale minerals depends on temperature and pressure. For instance, according to its thermodynamic data (thermodynamic database phreeqc.dat; Parkhurst and Appelo, 2013), barite solubility is reduced under lowered temperature and pressure conditions which are often accompanied by fluid production. Consequently, barite could be precipitated from formation water at saturation (saturation index=0; equilibrated) under decreasing pressure and temperature conditions within the producer.

(3) “Autoscale carbonate” formation at decreasing CO₂ partial pressure in producers and in their surrounding reservoir aquifer parallel to a drop in total pressure. This type of carbonate autoscale formation starts immediately after the onset of fluid production and pressure drawdown.

The chemical incompatibility between injected seawater and original formation water is the fundamental cause of potential hydrogeochemical reactions. Moreover, these reactions, which are thermodynamically driven, are coupled to and interact with the current hydraulic pore water flow. Thus, these three key factors (incompatibility, thermodynamics of chemical equilibrium, and water flow) lead to a new disequilibrium that tends to balance in

the form of massive dissolution and/or precipitation of minerals, including scale formation in different reservoir locations. In view of thermodynamics, injected seawater is commonly undersaturated with regard to several primary reservoir minerals in reservoir conditions. With respect to hydraulics, advection (characterized by flow velocities of formation water, seawater, or seawater–formation water mixtures) and longitudinal as well as transversal dispersion organize the transport of aqueous components through the reservoir aquifer. As a result, seawater and seawater–formation water mixtures, on one hand, completely replace the original and equilibrated formation water that previously occupied the pore space due to the hydraulic conditions established by seawater injection. This leads to re-equilibration which evolves along the flow paths from injectors to producers. On the other hand, pore water flow and coupled dispersion cause the mixing of aqueous components from both water types. Consequently, non-autoscaling (e.g., precipitation of sulfate minerals) appears within all reservoir parts and producers that are exposed to advective–dispersive compositional mixing of seawater and formation water. All simultaneous hydrogeochemical reactions are connected to each other and build a complex web of water–rock–gas interactions, including (1) proton-transfer reactions controlling pH, (2) electron-transfer reactions controlling redox conditions, (3) dissolution of unstable primary minerals, (4) precipitation of stable secondary minerals, (5) dissolution and outgassing of gases, (6) cation exchange, (7) surface complexation, and (8) irreversible reactions kinetically controlled (e.g., degradation of soluble crude oil components). All these processes convert and restructure the original mineralogical inventory at the aqueous–solid interfaces in the reservoir rocks. Concurrently, they alter the composition of erstwhile formation water, seawater, and multi-component gas, as well. Therefore, predictions in terms of the type and the intensity of subsequent wellbore scaling (non-autoscaling and autoscaling, as well) have to be built on considerations of the hydrogeochemical processes within the aquifer.

2. Scaling and formation damage: the engineer's perspective

According to the Schlumberger Oilfield Glossary (2015), scale is defined as a deposit or coating formed on the surface of metal, rock or other material; it may occur on wellbore tubulars and components. Formation damage is a term used by reservoir engineers to describe the reduction in permeability in the near-wellbore area of a reservoir. Among several other mechanisms, mineral precipitation in pore space is recognized as a chemical damage mechanism. Both wellbore scaling and formation damage may cause a strong reduction of productivity, finally leading to non-economic operations. Forecasting such production-interfering scaling and formation damage is high on the agenda for the successful reservoir engineering of offshore oilfields, but “not as straight forward as one might imagine” because of the complexity of such systems (Kan and Tomson 2011, p. 362; Fu et al., 2012).

Recently, Kan and Tomson (2011) presented an overview of the approaches applied by reservoir engineers to predict scale formation. Although based on the thermodynamics of chemical equilibrium for aqueous solutions, gaseous and solid phases, calculations of saturation indices (SI) for selected minerals are incapable of achieving the important demands for correctly evaluating scaling processes. SI calculations, which are based on the original composition of formation water and seawater, rule out the temporal and spatial development (1) of both water types and (2) of concurrent in-aquifer scaling and rock alteration by re-equilibration, as well. Thus, any modeling approach based on SI calculations is limited when reproducing or predicting scale formation due to several hydrogeochemical shortcomings (for details,

see [Fu et al., \(2013\)](#)) and its unrealistic concept. This also applies to zero-dimensional (“0D”) batch calculations, which also mix formation water and seawater and which provide the mass transfer via precipitation of scale minerals (e.g., the amount in mg l^{-1}) under equilibrium conditions (e.g., [Fu et al., 2012](#)). Most importantly, such approaches merely provide stand-alone approaches which cannot be embedded into three-dimensional geological and reservoir engineering modeling environments. This is due to the fact that such approaches exclude any temporal and spatial aspects. However, such approaches provide first insights into geosystems and show how the calculated composition of produced water could depend on the fraction of original seawater in mixtures with original formation water (both compositionally unaltered).

An alternative modeling approach is based – instead of numerical – on analytical solutions of governing equations for reactive flow. For instance, [Bedrikovetsky et al. \(2009\)](#) presented an analytical model of one-dimensional reactive flow in order to evaluate scaling processes. However, this model fails to reproduce realistic processes, because it ignores a complex web of chemical interactions and is restricted to the reaction between aqueous barium and sulfate ions to form barite. This analytical model ignores transversal and longitudinal dispersion, as well. Moreover, analytical approaches only provide a stand-alone solution for a defined system. Therefore, the results of such analytical approaches can not be embedded into the numerical, three-dimensional, finite element-based modeling environments used by geologists and/or reservoir engineers.

Recently, [Mackay et al. \(2012\)](#) presented their scaling-relevant modeling results by plotting (1) saturation ratios of barite and celestite (SrSO_4) versus seawater fraction, (2) saturation ratios versus time and water production rate, and (3) barium, strontium, and sulfate concentrations versus seawater fraction. This contribution by [Mackay et al. \(2012\)](#) lacks any quantitative modeling result about the spatial and temporal evolution of in-aquifer scaling, aquifer rock alteration, and wellbore scaling.

3. Bridging the gap: how hydrogeochemical modeling can connect geology and reservoir engineering

The geological concept of scale formation is based on investigation of the whole reservoir aquifer as a complex geosystem, and this concept includes the alteration of the mineral phase assemblage in reactive reservoir aquifers triggered by seawater injection. Consequently, such a view focuses on the spatial and temporal development of water–rock–gas interactions. The reservoir engineer’s perspective, instead, is inevitably focused on the successful injectivity and productivity of wellbores and on their near surroundings which are accessible to technical measures (e.g., scale inhibition). The porosity and permeability of reservoir rocks are two key factors affecting oil production. Mineral dissolution and precipitation affect most of the following parameters and their complex interplay which control the matrix permeability: pore size distribution, pore shape, connectivity, tortuosity, and specific surface. The clogging of pore throats by newly formed solid phases is an additional mechanism leading to a reduction in permeability ([Verma and Pruess, 1988](#)). In order to correctly evaluate the consequences of such processes, it is necessary to take into account that the slightest reductions in porosity which result from mineral precipitation can significantly reduce permeability. This is shown by laboratory experiments ([Vaughan, 1987](#)) and also by field data ([Pape et al., 2000](#)). Neither simple nor valid relationships to connect permeability to porosity are available. However, efficient water and scale management faces the challenge of a quantitative understanding (1) of scaling processes within wellbores and

reservoir aquifers, (2) of a concurrent reservoir rock alteration, and (3) of how these processes temporally and spatially evolve when seawater is injected.

The compositional incompatibility of injected seawater with original formation water and their mixing are the primary causes of scale formation in reservoir rocks. The composition of formation water can be attributed to the important inherent reservoir features, besides reservoir rock minerals, temperature–pressure conditions, and hydraulic properties of reservoir rocks (e.g., porosity, permeability, dispersivity). For example, [Wylde et al. \(2005\)](#) pointed out that seawater injection into the Miller oilfield created arguably the harshest oilfield-scaling regime in the North Sea (UK). According to their observations, barite dominated the scale mineral assemblage in the wellbores, besides celestite and calcite. This high intensity of Sr-barite scaling results from one of the inherent reservoir features of the Miller field – a high barium concentration in the formation water ([Lu et al., 2010](#); [Table S1](#)). In this contribution, we aim to unravel whether parameters that are controlled by a water injection strategy (e.g., injection and production rates, the spatial distribution of injectors and producers), can avoid “worst case” conditions for non-autoscale and/or auto-scale formation, such as the massive barite formation in the Miller field. For this, we applied numerical, finite element-based models that connect three-dimensional advective–dispersive pore water flow and reactive mass transport with the equilibrium thermodynamics of simultaneous chemical water–rock–gas interactions. Such three-dimensional reactive mass transport (3DRMT) models will therefore help to overcome the shortcomings of the state-of-the-art methods (e.g., SI-based calculations; analytical solutions of governing equations for reactive flow) in order to quantify the scaling risks. Moreover, they are capable of elucidating the temporal and spatial effects of seawater injection on reservoir rocks, formation water and gas, and consequently, could help to bridge the gap between three-dimensional geological models and the technical wellbore measures performed by reservoir engineers. Such an integrated understanding could help to adapt a water injection strategy to case-specific reservoirs in order to efficiently reduce the scaling intensity and to extend the wellbore life. Moreover, the promising application of 3DRMT modeling in our study provides a good example of how such an approach could support the water management of reservoir aquifers in view of seawater injection, injection of sulfate-reduced seawater or re-injection of produced water, or low salinity water flooding.

Our study focuses on diagenetic processes (including scale formation) driven by seawater injection and on their controlling factors. With this aim, we chose a reservoir aquifer that displays geochemical and hydrochemical characteristics which are similar to those observed in the Miller oilfield. This is because that the geochemical and hydrochemical characteristics (the mineralogy of the reservoir rocks and the composition of formation water and produced water) and the scaling processes of the Miller field have been well investigated in several studies ([Houston, 2007](#); [Houston et al., 2007](#); [Lu et al., 2010](#); [Fu et al., 2012, 2013](#)). However, it is not our aim to retrace or to reproduce the actual impact of seawater injection on the reservoir rocks and on scale formation in the Miller field. The hydraulic conditions in our study are established by varying different parameters which can be controlled by technical measures during injection (e.g., injectivity and productivity, the spatial distribution of injectors and producers).

4. Modeling setup and scenarios

The main methodology of our workflow is 3DRMT modeling by means of the PHAST computer code which is provided by the US Geological Survey (Water Resources Division; [Parkhurst et al.,](#)

2010). This computer code connects the hydrogeochemical computer code PHREEQC version 2.0 (Parkhurst and Appelo, 1999) with the three-dimensional groundwater flow and solute transport simulation code HST3D (Kipp, 1997). In our modeling approach of seawater injection, PHAST calculates the flow of the single fluid phase “formation water/injected seawater”. PHAST is a versatile groundwater flow and solute-transport simulator with capabilities to model a wide range of equilibrium and kinetic geochemical reactions (Parkhurst et al., 2010; p. 1). A large number of exemplary problems have been tested to confirm the numerical accuracy of the PHAST program for simulating coupled flow, transport, and chemical reactions by comparing results with analytical solutions, hand calculations, or published numerical results (Parkhurst et al., 2010; p. 131). Regarding the details of the governing equations and the mathematical techniques, we refer to the PHAST manual (Parkhurst et al., 2010; pp. 203–235). The related Model Viewer software (Hsieh and Winston, 2002) can be used to visualize the “four-dimensional” PHAST modeling results, and to evaluate them in a next step. A 3DRMT model using PHAST consists of a hydrogeochemical and a hydraulic part. For the hydrogeochemical part, we considered the conditions that have been identified in the Miller oilfield (Houston et al., 2007; Fu et al., 2012; for details, see Tables S1 and S2). In contrast, the hydraulic part of our 3DRMT model is of a generic nature. The hydraulic conditions are established by pre-assigning various parameters: some of them count for the reservoir rocks’ own properties (e.g., permeability distribution, dispersivity; Table S3); the remainder are controlled by the actual water injection strategy (e.g., spatial configuration of active producers and injectors; transient injection and production rates; Table S3). The hydraulic conditions, which are simplified and well-defined in our study, aim to show the general and dominating processes as well as the key factors that can strongly affect the intensity and the spatial distribution of scale formation. Thus, our model is of a semi-generic nature, but a good example of how to apply hydrogeochemical modeling for reservoir engineering.

4.1. Hydrogeochemical model part

Despite several limitations, the zero-dimensional (batch) modeling and the following one-dimensional reactive transport modeling of the processes in the Miller field (Fu et al., 2012, 2013) establish a fundamental basis for our complex 3DRMT model. Both studies provide a first insight into the type of hydrogeochemical reactions evolving in a siliciclastic reservoir undergoing seawater injection. The compositional development of the produced water (Houston, 2007) and the modeling results from Fu et al. (2012, 2013) demonstrate that seawater injection into the Miller oilfield indicates the following processes: (1) dissolution of calcite near injectors, and its precipitation within and near producers, (2) Sr-barite formation within producers and throughout the reservoir aquifer between injectors and producers, and (3) weak dissolution of microcrystalline quartz near injectors. Based on these findings, the reservoir rocks simulated in our study contain calcite, kaolinite and chalcedony as primary reactive minerals that may react with seawater or seawater–formation water mixtures. Although quartz is the predominant matrix component, it is handled as a non-reactive mineral in our model (Table S2; for details, see Fu et al. (2012, 2013)). Potential secondary minerals (barite, celestite, their solid solutions, anhydrite, witherite, strontianite, dolomite) can be precipitated from pore waters at saturation (Table S2). The injected seawater and the formation water (similar to that in the Miller field) prior to injection show a temperature of 4 °C and 120 °C, respectively (Table S1). Continued injection of relatively cold seawater can lead to a short-term cooling of reservoir rocks in the simulated reservoir aquifer. For the sake of simplicity, it is

assumed that a constant temperature and pressure of 80 °C and 500 bar prevail in the modeled reservoir aquifer over the total modeling time span of 10 years. Thus, wellbore-autoscaling, which is triggered by decreasing total pressure and temperature resulting from fluid production (e.g., sulfate autoscaling), remains unconsidered by our modeling due to the pre-assigned isothermal conditions at constant pressure within the producers.

The latest PHREEQC version (PHREEQC Interactive 3.0; Parkhurst and Appelo, 2013) and its thermodynamic database phreeqc.dat allow calculations of the effect of elevated total pressure conditions on the solubility equilibria of mineral phases, whereas the older PHREEQC version integrated in the PHAST computer code is restricted to a total pressure of 1 bar. In order to reduce this effect resulting from elevated pressure conditions, the solubility constants of chemically reactive minerals and gaseous CO₂ used in our study were separately calculated by using the PHREEQC Interactive 3.0 version for 500 bar and 80 °C (Table S2) and defined in the PHAST input file. In contrast, pressure effects on homogeneous reactions of aqueous species are ignored (for details, see Fu et al. (2012)). The 3DRMT model assumes that most parts of the reservoir aquifer are exposed to a *p*CO₂ of 10 bar at 80 °C under initial conditions prior to injection. Instead, a lower *p*CO₂ level of 5 bar (or 9 bar in an alternative scenario) is assumed to prevail in a pressure drop zone around the producer with a pre-assigned 5 m radius, and shall simulate the drop of the total pressure during production. With this exception, all other hydrogeochemical parameter values in the 3DRMT model aquifer are homogeneously distributed (Tables S1 and S2). Nevertheless, modeling with the PHAST computer code allows a heterogeneous distribution of geohydraulic and hydrogeochemical conditions provided that sufficient field data are available. Ion exchange and surface complexation are not considered by our study, because information about sorption capacities is lacking, and the effects of such sorption processes are assumed to be negligible. However, the computer code PHAST is capable of simulating sorption processes involving clay minerals or hydrous ferric oxides.

In summary, our 3DRMT modeling focuses on scale formation which is induced by the mixing of seawater with formation water. Furthermore, our modeling also integrates re-equilibration among injected seawater and reservoir rock mineral assemblages and also the formation of carbonate scales due to *p*CO₂ changes in a pressure drop zone near the producer, as well as in a zone where seawater characterized by a low *p*CO₂ flows into the reservoir aquifer with a higher *p*CO₂.

4.2. Hydraulic model part

The hydraulic part of our model is of a generic nature. For the sake of simplicity, the generic 3DRMT model describes (1) a homogenous distribution of the aquifer rock properties including porosity, permeability, dispersivity, and thickness, (2) steady-state flow conditions (constant rates of injection and production), and (3) constant hydraulic head and chemical boundary conditions for a confined reservoir aquifer (for details, see Tables S1 and S3). Our aquifer analog (the model) is composed of a 1000 m wide × 1000 m long × 50 m thick section as the reservoir aquifer beneath an oil column which is considered to be impermeable with regard to water. In the model, one central producer and four surrounding injectors penetrate the top five meters of the 50 m thick aquifer. They have a diameter of 1.0 m (including annulus). The generic 50 million m³ aquifer section is subdivided into 324,000 cells; each cell is 5.56 m long, 5.56 m wide and 5.0 m thick (corresponding to 180, 180, and 10 grid cells; Table S3). The following properties are assumed to be homogeneously distributed: (1) aquifer rock permeability of 1.0 Darcy (equivalent to ca. 0.000014 m s⁻¹ at reservoir conditions), (2) porosity of 0.14,

and (3) a dispersivity of 23, 2.3, and 0.2% of the grid cell length, width, and thickness for longitudinal, transversal-horizontal and vertical dispersion, respectively (Table S3). Our study focuses on chemical reactions, which proceed in oil reservoirs at all locations where dissolved chemical components of formation water and injected seawater may meet and react. The water leg, the oil-water transition zone, the oil-water contact, water within the oil leg, and even the water-wet mineral grains in the oil leg provide aqueous environments that may potentially be affected by such chemical reactions. Our modeling capabilities are restricted to the flow of water (single fluid flow in water-saturated porous media); the presence and the flow of oil are not considered by our modeling. In other words, oil is treated as a non-reactive component – in terms of hydrogeochemical reactions and geohydraulics, as well.

4.3. Modeling scenarios

In total, nine different scenarios are calculated with various values of the “non-inherent” reservoir parameters that are controlled by technical measures. They are (1) injection or production rates, (2) distances between injectors and the producer, and (3) $p\text{CO}_2$ drop due to the total pressure drawdown during fluid production. In all nine calculated scenarios, the “inherent” reservoir properties remain constant (Table 1). This study excludes biofilm formation, corrosion or completion brines, and also the migration of fines.

Scenarios “1” to “4” systematically modify the ratio of Total Injected Water Volume to Total Produced Water Volume (TIV/TPV) from 1:2 (8:16 Mio m^3) to 4:1 (8:2 Mio m^3). All other scenarios are sub-versions of scenario “2” and accordingly consider a TIV/TPV of 1:1. Scenarios “2.1” and “2.2” apply different injections rates of the four injectors (Maximum Injection Rate to Minimum Injection Rate; ratio $\text{IR}_{\text{max}}/\text{IR}_{\text{min}}$), whereas scenario “2” is based on equal injection rates. Further or closer distances between injectors and the producer are considered by scenarios “2.3” and “2.4”, while the distances are the same in scenario “2”. Scenario “2.5” applies a weaker CO_2 partial pressure drop in the producer from 10 bar to 9 bar instead of 5 bar (from 10 to 5 bar) in scenario “2”. This scenario aims to test the effect of the CO_2 partial pressure drop on the intensity of calcite autocalcification.

Scenario “2.P” resembles scenario “2” in terms of the applied hydraulic parameters, and is meant to evaluate the effects of different methods used for calculating high ionic strengths on the calculated hydrogeochemical mass transfer. This scenario “2.P” aims to test an alternative method to calculate aqueous ion activity coefficients at elevated levels of ionic strength (> 0.7 molal). The

“pitzer.dat” database, which is provided along with the “wateq4f.dat” database (Parkhurst and Appelo, 1999), enables us to calculate reliable ion activity coefficients at high ionic strengths (> 0.7 molal; Parkhurst and Appelo, 1999), but lacks some species (e.g., aluminum and silica species). Therefore, scenario “2.P” focuses on the behavior of Sr-barite, excludes the primary minerals kaolinite and chalcedony (cf. Table 1), and uses the “pitzer.dat” database.

5. Modeling results

We visualize the modeling results in the form of selected 3D figures from the originally animated (“4D”) Model Viewer visualization. A visualization of the spatial and temporal evolution of non-autoscale Sr-barite formation together with the evolution of seawater fractions is restricted to scenario “1” (Fig. 1). This highlights the spatial and temporal relationship between the pore water flow triggered by water injection and hydrogeochemical reactions thereby initiated (including scaling). The results from all other modeling scenarios are briefly described in Sections 5.2–5.5 and summarized in Table 2. The amounts of newly formed or dissolved minerals are given in cm^3 per 1.0 m^3 of porous reservoir rocks. One cubic meter of such porous aquifer rocks contains 140 l of pore space (original porosity: 0.14). We simplified the correct term “ cm^3 per 1.0 m^3 of porous aquifer rock” to “ cm^3 ” to indicate the amounts of newly formed or dissolved minerals.

5.1. Scenario “1”

After only 0.5 years of injection and during the transient stage of the seawater plume development, Sr-barite scaling (ca. 25 cm^3 ; Fig. 1a) emerges in wide areas of the plume, which is made up of seawater and its mixtures with formation water. In addition, cylindrical zones of Sr-barite formation develop within a distance of ca. 50 m around the injectors during this short period of time (Fig. 1b). In contrast, the injectors are free of any scale formation, even after ten years of injection (Fig. 1a–f).

After 1.0–1.5 years, weak Sr-barite scaling extends within the reservoir aquifer and reaches the producer, while the front of mixed water appears within the producers (Fig. 1b, c, h and i). Later, produced waters consist exclusively of different seawater-formation water mixtures that have compositionally developed within the aquifer (Fig. 1i–l). Longitudinal dispersive mixing dominates over transversal dispersive mixing during the early, transient stage of seawater plume development (Fig. 1g–i), while transversal dispersive mixing is the only mixing type under

Table 1
Modeling scenarios and various technical controllable parameter values.

| Scenario | TIV/TPV ^a ($\text{m}^3 \text{m}^{-3}$) | Injection rates ($\times 1000 \text{m}^3 \text{a}^{-1}$) | | | | Production rate ($\times 1000 \text{m}^3 \text{a}^{-1}$) | $p\text{CO}_2$ drop ^b (bar) | Distance of injector to producer (m) | | | |
|------------------|---|--|-------------|-------------|-------------|--|--|--------------------------------------|-----|-----|-----|
| | | I1 ^c | I2 | I3 | I4 | | | p ^d | I1 | I2 | I3 |
| 1 | 1/2 ^e | 200 | 200 | 200 | 200 | 1600 | 5 | 354 | 354 | 354 | 354 |
| 2 | 1/1 | 200 | 200 | 200 | 200 | 800 | 5 | 354 | 354 | 354 | 354 |
| 3 | 2/1 | 200 | 200 | 200 | 200 | 400 | 5 | 354 | 354 | 354 | 354 |
| 4 | 4/1 | 200 | 200 | 200 | 200 | 200 | 5 | 354 | 354 | 354 | 354 |
| 2.1 | 1/1 | 500 | 100 | 100 | 100 | 800 | 5 | 354 | 354 | 354 | 354 |
| 2.2 | 1/1 | 700 | 33.3 | 33.3 | 33.3 | 800 | 5 | 354 | 354 | 354 | 354 |
| 2.3 | 1/1 | 200 | 200 | 200 | 200 | 800 | 5 | 141 | 354 | 354 | 354 |
| 2.4 | 1/1 | 200 | 200 | 200 | 200 | 800 | 5 | 566 | 354 | 354 | 354 |
| 2.5 | 1/1 | 200 | 200 | 200 | 200 | 800 | 1 | 354 | 354 | 354 | 354 |
| 2.P ^f | 1/1 | 200 | 200 | 200 | 200 | 800 | 5 | 354 | 354 | 354 | 354 |

^a Ratio of Total Injected Water Volume (TIV) to Total Produced Water Volume (TPV).

^b Difference in $p\text{CO}_2$ between reservoir aquifer and producer.

^c Four injectors, in total (I1 to I4).

^d One central producer.

^e Bold: Parameter values modified compared to scenario 2.

^f The pitzer.dat database is applied to scenario 2.

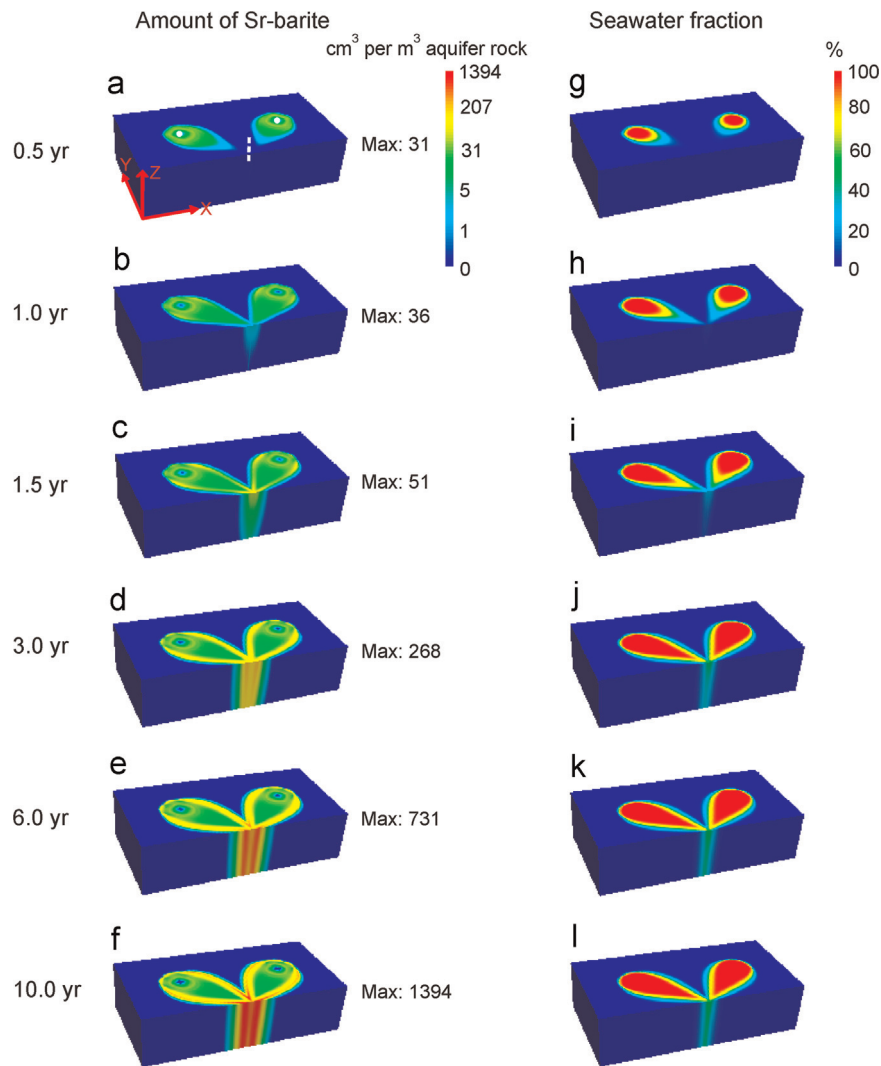


Fig. 1. Modeled temporal and spatial distribution of Sr-barite and of seawater fractions after 0.5 up to 10.0 years of seawater injection for scenario “1”. Cross section through the central producer: $1000 \text{ m} \times 500 \text{ m} \times 50 \text{ m}$ (in x , y , and z directions; red arrows in (a)); the central producer: white dashed line in (a); two (of four) injectors: white dots in (a); max: maximum amount.

steady-state conditions. Later (> 3.0 years in scenario “1”), the compositional development of the seawater plumes reaches a steady state and mixing is restricted to the margins of the seawater plumes (Fig. 1j–l). Additional Sr-barite formation starts at the margins of the seawater plumes with seawater fractions of ca. 35–40% after 1.0 years (Fig. 1b–f). With ongoing injection, the content of Sr-barite scale formed within these zones increases, and finally reaches 1394 cm^3 at maximum (after 10 years; Fig. 1d–f). Sr-barite formation peaks at seawater plume margins that approach and converge close to the producer – at a distance of some tens of meters (Figs. 1e and f, and 2a–d).

At the location of the producer, Sr-barite formation ($> 25 \text{ cm}^3$; arbitrarily chosen; dominantly $\text{Sr}_{0.02}\text{Ba}_{0.98}\text{SO}_4$) starts ca. 1.5 years after the onset of water injection (Fig. 1b and c). At this time, a water mixture containing ca. 25% seawater occupies the pore space of the aquifer close to and at the location of the producer (Fig. 1h and i). After ten years, 500 cm^3 of Sr-barite newly forms within the producer (Table 2; Fig. 1f), and lowers the concentration of barium and sulfate ions. Consequently, the formation waters calculated in all scenarios are always undersaturated with regard to barite, celestite, and anhydrite. Sr-barite is the single sulfate-bearing mineral precipitated in all scenarios.

Immediately after the onset of production, isothermal calcite

autoscaling starts within the pressure drop zone at the producer (5 m radius, pre-assigned). After 10 years, the amount of calcite scale reaches 2140 cm^3 (scenario “1”; Table 2). In addition and similar to Sr-barite, smaller amounts of non-autoscale calcite (ca. $100\text{--}500 \text{ cm}^3$) form at those cross-shaped margins of seawater plumes that approach and converge close to the producer. In contrast, primary calcite (initially $16,850 \text{ cm}^3$) gets completely dissolved within a radius of ca. 40 m around all four injectors after 10 years of seawater injection (Table 2; Fig. S1). At the expense of calcite, dolomite newly forms in these aquifer areas close to the injectors ($11,000 \text{ cm}^3$ after 10 years; Table 2; Fig. S1).

Similar to calcite, the primary mineral phase chalcedony dissolves in the injected seawater – until these reactions reach the “new” state of chemical equilibrium. These chalcedony coatings (100 cm^3) completely dissolve in areas stretching over ca. 45 m around the injectors during ten years of injection (Fig. S1). Meanwhile, small amounts of the primary kaolinite inventory (ca. 20 from 8700 cm^3) dissolve close to the injectors (no details presented here). Neither anhydrite nor gypsum forms as secondary non-autoscales within the aquifer or within the production wellbores in all scenarios.

Table 2
Modeling results.

| Scenario | Scale formation | | | | | | Aquifer rock alteration | | | Technical measures | | | |
|--|-------------------------|--|---------------------------------|---|---------------------|---|----------------------------------|---|----------------|----------------------|---|--------------------------|-----------------------|
| | In production well (PW) | | in aquifer near PW | | | | Close to injectors after 10 a | | | TIV/TPV ^a | IR _{max} /IR _{min} ^b | DI-1/DI-234 ^c | pCO ₂ drop |
| | Sr-barite ^d | Calcite formed | maximum of Sr-barite after 10 a | | dissolved Calcite | Dolomite formed | | | | | | | |
| Highest amount after 10 a cm ³ m ⁻³ | Begin Year | Highest amount after 10 a cm ³ m ⁻³ | Begin Year | Amount cm ³ m ⁻³ | Distance to PW m | Highest amount cm ³ m ⁻³ | Zone around PW ^e m | Highest amount cm ³ m ⁻³ | - ^f | - | - | bar | |
| 1 | 500 | 1.5 | 2140 | < 0.1 | 1394 | 22–35 | 16,850 | 40 | 11,000 | 1/2 | 1/1 | 1/1 | 5 |
| 2 | 200 | 2.5 | 1610 | < 0.1 | 482 | 28–50 | 16,850 | 40 | 11,000 | 1/1 | 1/1 | 1/1 | 5 |
| 3 | 80 | 4.0 | 1850 | < 0.1 | 222 | 17–40 | 16,850 | 40 | 11,000 | 2/1 | 1/1 | 1/1 | 5 |
| 4 | 70 | 6.0 | 2390 | < 0.1 | 166 | 10–35 | 16,850 | 40 | 11,000 | 4/1 | 1/1 | 1/1 | 5 |
| 2.1 | 400 | 2.0 | 1690 | < 0.1 | 797 | 25–45 | 16,850 | 28 and 55 | 11,000 | 1/1 | 5/1 | 1/1 | 5 |
| 2.2 | 750 | 1.5 | 1972 | < 0.1 | 796 | 0–10 | 16,850 | 28 and 95 | 13,000 | 1/1 | 21/1 | 1/1 | 5 |
| 2.3 | 550 | < 0.5 | 1480 | < 0.1 | 776 | > 100 | 16,850 | 40 | 11,100 | 1/1 | 1/1 | 0.4 | 5 |
| 2.4 | 500 | 2.5 | 1950 | < 0.1 | 861 | < 5–17 | 16,850 | 40 | 11,000 | 1/1 | 1/1 | 1.6 | 5 |
| 2.5 | 200 | 2.5 | 400 | < 0.1 | 482 | 28–50 | 16,850 | 40 | 11,000 | 1/1 | 1/1 | 1/1 | 1 |

^a Ratio of Total Injected Water Volume (TIV) to Total Produced Water Volume (TPV).

^b Ratio of maximum injection rate to minimum injection rate (IR_{max}/IR_{min}) among different injectors; see Table 1.

^c Ratio of distances between injector and producer.

^d Sr-barite is the single sulfate-bearing mineral newly formed in all scenarios, whereas the other sulfate-bearing minerals (potential secondary minerals) show a negative saturation index.

^e Maximum radius of complete dissolution of calcite.

^f Dimensionless.

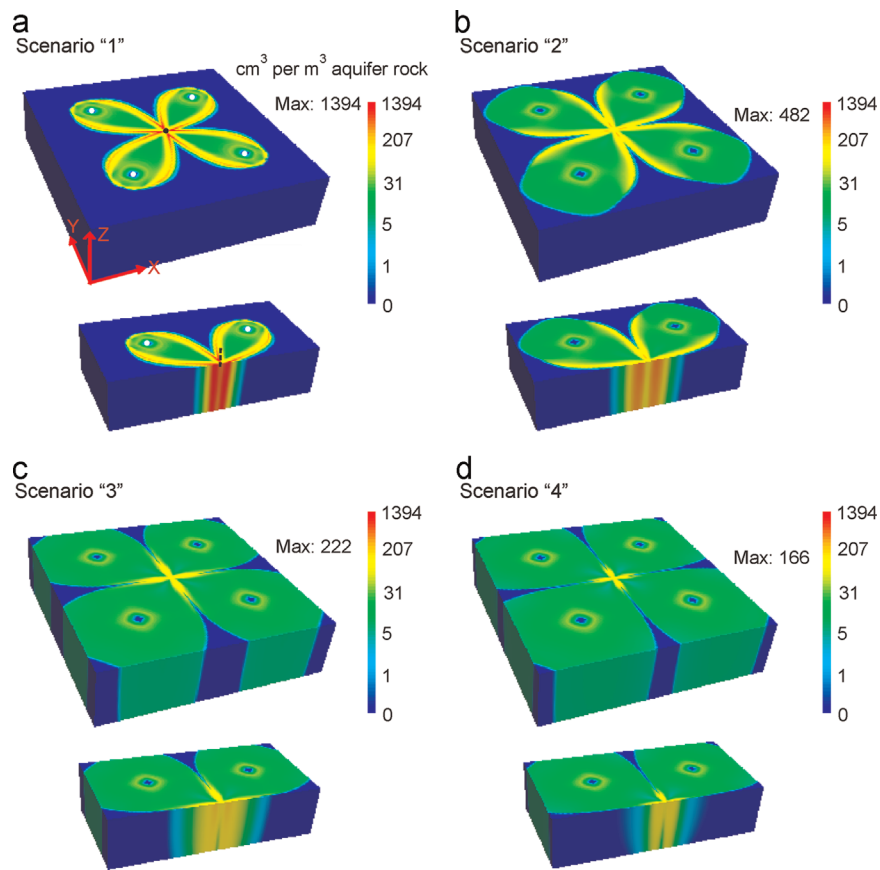


Fig. 2. Modeled spatial distribution of Sr-barite after 10 years of seawater injection for scenarios “1”, “2”, “3”, and “4”. Whole aquifer section: 1000 m × 1000 m × 50 m (in x, y, and z directions; red arrows in (a)); one central producer: black dot and black dashed line in (a); four (or two) surrounding injectors: white dots in (a); max: maximum amount.

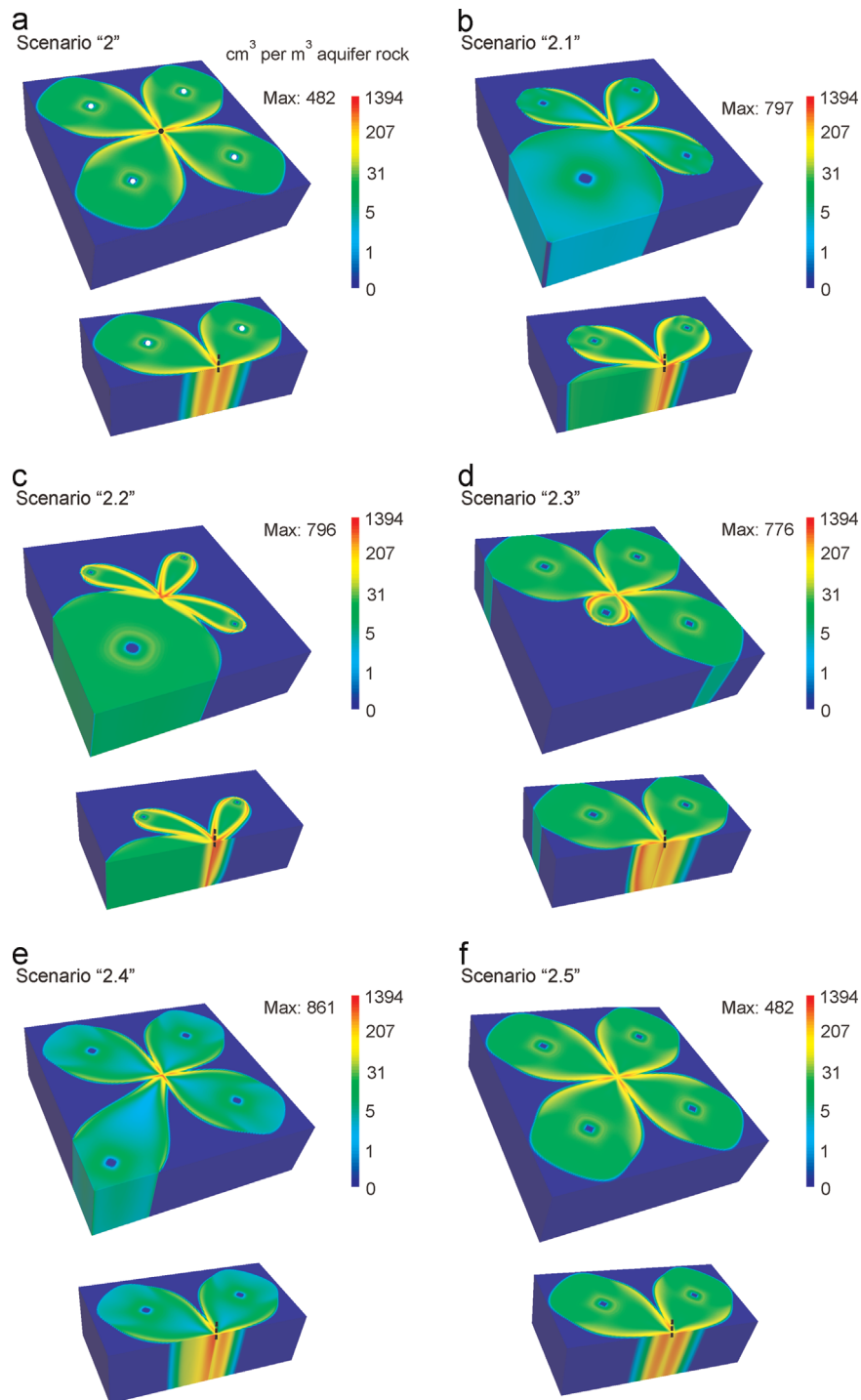


Fig. 3. Modeled spatial distribution of Sr-barite after 10 years of seawater injection for scenarios “2” to “2.5”. One central producer: black dashed line or black dot in (a); two (of four) injectors: white dots in (a); max: maximum amount.

5.2. Effects of TIV/TPV ratio

The ratio of Total Injected Water Volume to Total Produced Water Volume (TIV/TPV) is one of the parameters that are controlled by technical measures and which can significantly affect the hydraulic conditions in the reservoir aquifer during water injection. Scenarios “1” to “4” modify this ratio from 1:2 to 4:1 over ten years of injection (Table 2). The modeling results show that areas of intense Sr-barite formation, independent of the TIV/TPV ratio, generally appear at the margins of the seawater plumes, and that Sr-barite scaling is more or less uniformly distributed in the

central parts of these plumes (Fig. 2). The injectors are free of scaling in all scenarios, whereas a cylindrical zone of barite scaling develops around the injector within a greater distance of ca. 50 m after ten years (Fig. 2). The areas of most Sr-barite formation emerge in those marginal seawater plume regions that approach and converge close to the producer (Fig. 2). In other words, the location of the producer itself is not the hot-spot of non-autoscale Sr-barite formation. Formation of non-autoscale Sr-barite at the producer (scenarios “1” to “4”) reaches only ca. 50% of the maximum amount of Sr-barite formed in the near-surrounding reservoir rocks of the producer (Fig. 2; Table 2). Although the

wellbore penetration depths are limited to the top five meters of the aquifer, Sr-barite precipitation covers the entire aquifer thickness of 50 m in all modeling scenarios (Fig. 3).

An increase in the TIV/TPV ratio leads to decreasing differences in the hydraulic head between the injectors and the producer: from 27 bar in scenario “1” to 6 bar in scenario “4”. Thus, seawater flows more quickly and reaches the producer earlier in scenario “1” compared to scenario “4”. Accordingly, non-autoscale Sr-barite formation within the producer occurs earliest in scenario “1”, already after 1.5 years, when compared to 2.5, 4.0, and 6.0 years in scenarios “2” to “4”, respectively (Table 2).

Regarding the spatial aspect, a decreasing TIV/TPV ratio spatially restricts Sr-barite formation. Sr-barite forms in ca. 40 vol% of the total reservoir aquifer in scenario “1” with a TIV/TPV ratio of 1:2 compared to 90 vol% of the reservoir aquifer in scenario “4” with a ratio of 4:1 (after 10 years; Fig. 2). In contrast, an increase in TIV/TPV ratio reduces Sr-barite formation, not only within the producer, but also in the whole reservoir aquifer. The most intense formation of Sr-barite appears in scenario “1” with the lowest TIV/TPV ratio in the four scenarios: at maximum 500 and 1394 cm³ of Sr-barite within the producer and in the reservoir close to the producer (Table 2; Fig. 2).

Although the same drop in $p\text{CO}_2$ (5 bar) is applied for scenarios “1” to “4”, the amount of newly formed calcite autoscale after 10 years varies with the applied TIV/TPV ratio: from 2140 cm³ (scenario “1”), to 1610, to 1850, and to 2390 cm³, respectively (scenarios “2” to “4”). In contrast, the behavior of calcite, dolomite (Table 2), chalcedony and kaolinite close to injectors is independent of the TIV/TPV ratio.

5.3. Effects of injection rates – IR_{\max}/IR_{\min} ratio

Scenarios “2”, “2.1”, and “2.2” consider a constant production rate, but vary the IR_{\max}/IR_{\min} ratio (Maximum Injection Rate to Minimum Injection Rate) from 1:1, 5:1, and finally to 21:1 (Table 1). Changing the IR_{\max}/IR_{\min} ratio is restricted to an increase in the injection rate of one injector and concurrently to a decrease in the injection rate of the other three injectors, whereas the total injection rate of all four injectors remains constant compared to scenario “2”. Comparing the modeling results from these three scenarios shows that increasing the IR_{\max}/IR_{\min} ratio leads to more intense Sr-barite formation within the producer: 200, 400, 750 cm³, respectively (Table 2; Fig. 3a–c). At the highest IR_{\max}/IR_{\min} ratio in scenario “2.2”, Sr-barite scaling within the producer begins earliest, while the most calcite scale newly forms within the producer (Table 2). In total, more Sr-barite newly forms in the reservoir aquifer of scenarios “2.2”, and this higher scaling appears closer to the producer than in scenario “2” (Table 2; Fig. 3a and c). However, the various IR_{\max}/IR_{\min} ratios barely affect the behavior of calcite dissolved and dolomite formed near the injectors (Table 2).

5.4. Effects of spatial arrangement of injectors and producers – DI-1/DI-234 ratio

Scenarios “2”, “2.3”, and “2.4” aim to investigate the effects of the spatial arrangement of injectors and producers on scale formation. They conceptually vary the distance between one of the four injectors and the producer (DI-1), while the distances of the other three injectors to the producer remain constant (DI-2=DI-3=DI-4; abbreviated as DI-234). The ratio of the distance between the injectors and the producer is described as the DI-1/DI-234 ratio (Table 2). Scenario “2” is calculated based on a constant distance of all four injectors to the producer (DI-1=DI-234=354 m, in other words, DI-1/DI-234 ratio=1; Tables 1 and 2). In comparison, scenarios “2.3” and “2.4” reduce and increase DI

to 141 m and to 566 m, respectively (Table 1). Accordingly, the DI-1/DI-234 ratio of both these scenarios is changed to 0.4 and to 1.6, respectively (Table 2). The lowest DI-1/DI-234 ratio (the shortest distance between the producer and one of the injectors) leads to the earliest and most intense precipitation of Sr-barite in the producer (<0.5 year and 550 cm³ in scenario 2.3; Table 2). Moreover, a lower DI-1/DI-234 ratio keeps the most intensive Sr-barite formation far from the producer: a distance of >100 m between the producer and the location with the most Sr-barite in scenario “2.3” compared to a distance of <5 m in scenario “2.4” (Table 2; Fig. 3d and e). In contrast, the DI-1/DI-234 ratio hardly affects the intensity of calcite scaling within the producer, or of calcite dissolution and dolomite precipitation in the reservoir aquifer near the injectors (Table 2).

5.5. Consequences of decreasing $p\text{CO}_2$

A fall in $p\text{CO}_2$ within the producer and in its surroundings often occurs during production, and it can consequently cause strong carbonate autoscaling. Scenarios “2” and “2.5” pre-assume two different $p\text{CO}_2$ declines. Calcite autoscale forms to a very much smaller degree within the pressure drop zone at the location of the production well (400 cm³) when a smaller drop in $p\text{CO}_2$ of 1 bar is applied in scenario “2.5” instead of 5 bar in scenario “2” (Table 2). Comparison of the results calculated by scenarios “2” and “2.5” shows that the other parameters (e.g., Sr-barite scaling, the amount of dolomite precipitated near the injectors) are insensitive to the $p\text{CO}_2$ drop in the producer.

An alternative scenario “2.P” uses the thermodynamic database pitzer.dat and aims to evaluate the effects of different methods for calculating high ionic strengths on the calculated intensity and spatial distribution of scale formation. The modeling results of scenario “2.P” resemble the results of scenario “2” (Table 2).

6. Discussion

6.1. Close relationship between Hydraulic processes and scale formation

Conceptually, the total volume of injected seawater determines the maximum amount of scale minerals that can potentially form. However, hydraulic processes can spatially distribute such scale formation, and consequently control its local intensity. In our case study, Sr-barite is precipitated as non-autoscale during seawater injection. Here, for the sake of simplicity, we use Sr-barite as a representative for all other non-autoscale minerals. Formation of Sr-barite is triggered by mixing different water components due to an Sr-barite oversaturation. Consequently, Sr-barite appears in flow-field areas of dispersive mixing of seawater and formation water. In addition, Sr-barite also forms close to and in the producer where water components with different seawater fractions (correspondingly different activities of barium, strontium and sulfate) are admixed, although these components were previously equilibrated with Sr-barite.

Longitudinal dispersion triggers Sr-barite formation within growing seawater plumes. Seawater moving towards the producer displaces the (mobile) formation water along its moving front. Such longitudinal dispersive mixing at this front is restricted to the transient stage of the plume development; it proceeds as long as seawater displaces formation water within the expanding seawater plume. This in-plume Sr-barite scaling driven by longitudinal dispersion stops when the seawater plume reaches the producer and seawater completely occupies the pore space within the inner core of the plume (Fig. 1).

The second dispersive mixing process is transversal dispersion;

it occurs at the margins of seawater plumes which are surrounded by formation water. In contrast to longitudinal dispersion, such transversal mixing of seawater and formation water causes in-aquifer Sr-barite formation during the transient stage and also under steady-state conditions of mass transport, and still proceeds after “seawater breakthrough” at the producer (Fig. 1). Dispersive mixing controls the evolution of Sr-barite formation at the margins of seawater plumes at moderate seawater fractions. Consequently, the producer focuses the fluxes of dissolved barium and strontium (both originated from formation water) and sulfate (originated from seawater). However, after seawater breakthrough at the producer, the production waters are seawater–formation water mixtures that have already undergone compositional alteration along their pathways through the aquifer via water–rock–gas interactions. Such mixtures are depleted in their barium, strontium and sulfate contents to a certain level via in-aquifer Sr-barite formation. Therefore, the producer itself, which is the ultimate mixing site, is not the location of most non-autoscale formation. The combined effects of (1) converging margins of seawater plumes, (2) focused fluxes, and (3) continuous mixing during the transient stage and also under steady-state conditions determine the “hot spot” of non-autoscale formation. It is located at those cross-shaped margins of neighboring seawater plumes and of their peripheral mixtures with formation water that approach and converge in the near-surroundings of the producer, some tens of meters away from the producer (Fig. 2).

In summary, our modeling results show a coupling and an interacting relationship between hydraulic transport processes and hydrogeochemical reactions including scale formation. Hydraulic processes are the key for the temporal and spatial development of scale formation, because they determine the mixing of incompatible water types in time and space. Moreover, hydraulic processes can locally intensify non-autoscaling in the reservoir aquifer (e.g., Sr-barite in our case study). On the other hand, they can further mitigate the scaling severity in other reservoir parts. Hydraulic processes are complex due to a broad variety of inherent reservoir features (e.g., heterogeneous distribution of porosity and permeability) and also of technical measures (e.g., spatial configuration of injectors and producers, injectivity). Thus, zero-dimensional modeling approaches, which are based only on the mixing of injected seawater and original formation water without any temporal and spatial aspects, are incapable of evaluating the scaling intensity. In contrast, 3DMT modeling should be used to correctly predict the temporal and spatial tendencies of scaling for successful water and scale management.

6.2. Complexity of water–rock–gas interactions

The chemical incompatibility of injected seawater and original formation water is the primary cause of scale formation in reservoirs. On the other hand, this incompatibility exactly reflects that injected seawater is commonly undersaturated with respect to several primary minerals in reservoirs under elevated reservoir temperature and pressure conditions. Consequently, seawater injection alters reservoir rocks near injectors. In parallel, the chemical composition of the injected seawater changes. Such changes will directly affect the severity of scaling formation, when altered seawater is admixed to formation water within producers. For instance, the injected seawater is undersaturated with calcite in our study due to a high $p\text{CO}_2$ in the reservoir. Therefore, a re-equilibration among injected seawater, minerals (including calcite), and CO_2 -rich gas leads to a complete dissolution of primary calcite within a distinct radius around the injectors. Our modeling starts from the assumption that the primary calcite of the rock matrix is completely exposed to the seawater or to its mixtures with formation water. This might not be the case in all real

reservoir systems. In consequence, the dissolution zone of primary rock minerals around the injectors would even be larger, but less intense. Such dissolution of primary rock minerals, however, depends on the mineral content, the hydraulic conditions, the duration of injection, and also on the hydrogeochemical conditions in reservoirs (e.g., reservoir temperature, $p\text{CO}_2$).

Dissolution of primary rock minerals around injectors could enhance porosity and permeability. On the other hand, aqueous ions are released by mineral dissolution into seawater or its mixtures with formation water and transported along the flow path through the reservoir aquifer. Such interacting hydrogeochemical and hydraulic processes result in an oversaturation of altered seawater or its mixtures with regard to specific minerals at different reservoir location and in local scaling. Taking our case study as an example, dolomite is newly formed at the expense of calcite in the areas close to the injectors (Table 2). However, its formation does not fully bind all calcium ions released by calcite dissolved from the reservoir rocks (e.g., $16,850 \text{ cm}^3 \text{ m}^{-3}$ of dissolved calcite and $11,000 \text{ cm}^3 \text{ m}^{-3}$ of precipitated dolomite in scenario “1”; Table 2). The excess of calcium ions is sequestered by the subsequent calcite formation as in-aquifer non-autoscale in the reservoir rocks and by calcite autoscaling in producers. This demonstrates that hydrogeochemical water–rock–gas reactions are integrated into a complex web and are connected in process series. More importantly, our modeling results reveal that a generalization about mineral behavior (dissolution or precipitation) is inadequate for evaluating scale formation. This is due to the fact that even the same mineral can respond differently to seawater injection at different reservoir locations. Thus, zero-dimensional modeling approaches and calculations of saturation indices of selected minerals even by using a transport model are incapable of correctly reproducing hydrogeochemical processes including scaling.

6.3. Effects of technically controlled parameters

Several key parameters that can be technically controlled for managing seawater injection have been considered by various modeling scenarios. They are (1) the TIV/TPV ratio, (2) the $\text{IR}_{\text{max}}/\text{IR}_{\text{min}}$ ratio among various injectors, (3) the distance between injectors and the producer (DI-1/DI-234 ratio), and (4) the drop in $p\text{CO}_2$ (Table 1). Although hydrogeochemical processes including scale formation are an inevitable result of seawater injection due to the incompatibility of seawater and formation water, our modeling results show that such technically controlled parameters can significantly affect the intensity, and the temporal and spatial development of scale formation.

An increase in the TIV/TPV ratio mitigates and retards the formation of non-autoscale minerals within producers (Sr-barite formation in scenario “1”, “2”, “3”, and “4”; Table 2). In parallel, it leads to weaker non-autoscaling in the reservoir aquifer close to producers. Similarly, unequal injection rates of various injectors and/or an asymmetrical spatial configuration of injectors (an increase in $\text{IR}_{\text{max}}/\text{IR}_{\text{min}}$ ratio and/or in DI-1/DI-234 ratio) enhance the severity of non-autoscaling in the reservoir aquifer near to and in the producer itself (scenarios “2.1” to “2.4”). Moreover, the three key parameters (TIV/TPV ratio, $\text{IR}_{\text{max}}/\text{IR}_{\text{min}}$ ratio, DI-1/DI-234 ratio) also control the time span after which massive non-autoscale formation starts at the location of the producer. These time spans can vary by a factor of 12 at maximum under the tested hydraulic conditions. In consequence, 3DRMT modeling can help reservoir engineers to identify an optimal combination of TIV/TPV, $\text{IR}_{\text{max}}/\text{IR}_{\text{min}}$, and DI-1/DI-234 in order (1) to force scaling to preferentially develop within the aquifer rock – instead of close to or within wellbores, (2) to retard scaling within wellbores, and (3) to minimize the severity of scaling within wellbores.

Formation of carbonate autoscales is induced within the $p\text{CO}_2$ drop zone around the producer. A greater $p\text{CO}_2$ drop strongly intensifies carbonate formation within the producer (compare scenario “2” to “2.5”; Table 2). An alternative scenario “2.P” uses the pitzer database to consider a high ionic strength which is often observed in the formation water. The modeling results show that the method to calculate aqueous ion activity coefficients at elevated levels of ionic strength is not a key factor for the calculated amounts of Sr-barite scale.

The PHAST/PHREEQC modeling environment is capable of including reaction kinetics (e.g., of precipitation/dissolution reactions; irreversible redox reactions like anoxic oil degradation; Parkhurst et al., 2010), which have not been considered by our modeling so far. Nevertheless, appropriate rate constants for such reactions are basic prerequisites and should be applicable in case-specific reservoir conditions. Provided that such rate constants are available, even sulfate reduction by aqueous, degradable oil-derived organic carbon components (anoxic oil degradation driven by sulfate influx into the oil–water transition zone) may be included in our 3DRMT modeling. Consequently, the effects of sulfate reduction on sulfate scaling, on aquifer rock alteration (e.g., formation of sulfide/di-sulfide mineral phases), and on potentially evolving H_2S partial pressures could be integrated in our modeling approach. This holds true also for technical measures to suppress sulfate reduction and H_2S formation by the addition of nitrate as an oxidant competing with sulfate.

6.4. Modeling limitations

Our modeling is conceptually based on isothermal and constant total pressure conditions in the aquifer, within the plume of injected seawater, and within the producer and the injectors, as well. Therefore, the modeled scale formation is exclusively of the non-autoscale type, which results from compositional mixing of seawater and formation water.

Several factors were not addressed by our modeling. Such factors can affect the calculated amount and spatial-temporal distribution of scale formation. They are (1) mass fluxes between mobile pore water (seawater or seawater–formation water mixtures) and immobile (irreducible) pore water, and (2) numerical dispersion which may cause a spatial “smearing” of the modeled results.

The spacing of grid blocks and the size of time steps applied in our model (its discretization) also affect the calculated amount of minerals that newly form or dissolve. However, all of our modeling scenarios use the same discretization. Therefore, we compare the modeling results rather than discussing and evaluating absolute numbers.

7. Conclusions

The three-dimensional reactive mass transport (3DRMT) modeling of seawater injection into a semi-generic reservoir aquifer highlights how hydrogeochemical and interconnected hydraulic processes control the spatial and temporal development of (1) thereby triggered diagenetic water–rock–gas interactions (re-equilibration), (2) in-aquifer scaling, and (3) production wellbore scaling.

The flow of injected seawater and formation water controls their advective and dispersive mixing throughout the reservoir aquifer from injectors to producers. Consequently, the modeling results show that different reservoir parts differ in their mixing factors, which change during water injection. Thus, the intensity of non-autoscaling in the reservoir varies, for instance, Sr-barite formation in our case study. Moreover, the calculated results

reveal that the producer itself, which is the ultimate mixing site, is not the “hot spot” of the most intense non-autoscaling. A combination of different mass transport processes focuses non-autoscaling formation at the cross-shaped margins of neighboring seawater plumes and at their peripheral mixtures with formation water that approach to and converge in the near-surroundings of the producer, some tens of meters away from the producer.

Scaling is a thermodynamically inevitable consequence of seawater injection. However, several parameters that are technically manageable can strongly affect the spatial and temporal development of scaling processes, especially of non-autoscaling: (1) the ratio of Total Injected Water Volume to Total Produced Water Volume (TIV/TPV), (2) the ratio of Maximum Injection Rate to Minimum Injection Rate ($\text{IR}_{\text{max}}/\text{IR}_{\text{min}}$) among various injectors, and (3) the distance between injectors and producers (DI-1/DI-234). They can mitigate and retard the formation of scale minerals close to and in producers. In consequence, reservoir engineers aiming to extend wellbore life by minimizing non-autoscale and autoscale formation (e.g., Sr-barite) are enabled by 3DRMT modeling to identify those hydraulic conditions of injection (TIV/TPV, $\text{IR}_{\text{max}}/\text{IR}_{\text{min}}$, DI-1/DI-234) that force scale minerals preferentially precipitated within the aquifer rock – instead of close to or within the well bore.

Several alternative approaches to forecast the “scaling tendencies” of producers, calculate (1) “pure end member mixing” of compositionally unaltered seawater and formation water in zero-dimensional reactors, or (2) saturation indices by using transport models. Such approaches are incapable of correctly predicting scaling processes. This is because, as shown by our 3DRMT modeling, unaltered seawater will not reach the producer to mix.

In addition to scale formation in producers and throughout the surrounding reservoir, seawater injection induces several hydrogeochemical processes in the reservoir aquifer close to injectors due to re-equilibration between injected seawater, reservoir rocks, and co-existing reservoir gases. Such processes are the thermodynamically inevitable consequence of the reactive nature of the reservoir aquifer. This re-equilibration leads to the dissolution of primary unstable minerals and to the formation of secondary stable minerals in the surroundings of injectors after the onset of seawater injection. It not only restructures the reservoir rock matrix with respect to mineralogy, and thus, the porosity and permeability close to injectors, but also alters the composition of the injected seawater that later flows into producers and is admixed into formation water. The dissolution of primary minerals provides ionic components of scale formation in producers. Moreover, such modeling results show that all water–rock–gas interactions – including scaling – are integrated in a complex web of interactions and are coupled to the flow of pore water. They are a mandatory key to predict scaling.

Thus, we recommend applications of case-specific 3DRMT modeling of seawater injection in order to test different possible hydraulic conditions and to thereby identify (among other parameters) the hydraulic configurations that can avoid “worst case” conditions with respect to the amount and timing of scaling processes. Additionally, such 3DRMT modeling will help to optimize efficient scale inhibition measures, especially when this 3DRMT modeling tool is integrated in geological and reservoir engineering model environments.

Acknowledgments

We thank Steffen Häußler for his support in performing PHAST modeling.

Appendix A. Supplementary material

Supplementary data associated with this article can be found in the online version at <http://dx.doi.org/10.1016/j.petrol.2015.09.014>.

References

- Bader, M.S.H., 2007. Sulfate removal technologies for oil fields seawater injection operations. *J. Pet. Sci. Eng.* 55, 93–110. <http://dx.doi.org/10.1016/j.petrol.2006.04.010>.
- Bedrikovetsky, P.G., Mackay, E.J., Silva, R.M.P., Patricio, F.M.R., Rosário, F.F., 2009. Produced water re-injection with seawater treated by sulphate reduction plant: injectivity decline, analytical model. *J. Pet. Sci. Eng.* 68, 19–28. <http://dx.doi.org/10.1016/j.petrol.2009.05.015>.
- Crabtree, M., Eslinger, D., Fletcher, P., Miller, M., Johnson, A., King, G., 1999. Fighting scale – removal and prevention. *Oilfield Rev.* 11, 30–45 (Autumn 1999).
- Ehrenberg, S.N., Jakobsen, K.G., 2001. Plagioclase dissolution related to biodegradation of oil in Brent Group sandstones (Middle Jurassic) of Gullfaks field, northern North Sea. *Sedimentology* 48, 703–721. <http://dx.doi.org/10.1046/j.1365-3091.2001.00387.x>.
- Fu, Y., van Berk, W., Schulz, H.-M., 2012. Hydrogeochemical modelling of fluid–rock interactions triggered by seawater injection into oil reservoirs: case study Miller field (UK North Sea). *Appl. Geochem.* 27, 1266–1277. <http://dx.doi.org/10.1016/j.apgeochem.2012.03.002>.
- Fu, Y., van Berk, W., Schulz, H.-M., 2013. Temporal and spatial development of scale formation: one-dimensional hydrogeochemical transport modeling. *J. Pet. Sci. Eng.* 112, 273–283. <http://dx.doi.org/10.1016/j.petrol.2013.11.014>.
- Guan, L., Du, Y., Wang, Z., Xu, W., 2005. Water injectivity – what we have learned in the past 30 years. *J. Can. Pet. Technol.* 45, 9–13.
- Houston, S.J., 2007. Formation Waters in Petroleum Reservoirs: Their Controls and Applications (Ph.D. Thesis). University of Leeds, England, pp. 69–92, Appendix V (March 2007).
- Houston, S.J., Yardley, B.W.D., Smalley, P.C., Collins, I., 2007. Rapid fluid–rock interaction in oilfield reservoirs. *Geology* 35, 1143–1146.
- Hsieh, P.A., Winston, R.B., 2002. User's guide to model viewer – a program for three-dimensional visualization of groundwater model results. U.S. Geological Survey, Open-File Report 02-106. p. 18.
- Kan, A.T., Tomson, M.B., 2011. Scale prediction for oil and gas production. In: Proceedings of CPS/SPE International Oil & Gas and Exhibition. Society of Petroleum Engineers (SPE 132237), 8–10 June 2011. Beijing, China.
- Kipp, K.L. Jr., 1997. Guide to the Revised Heat and Solute Transport Simulator HST3D – Version 2. U.S. Geological Survey, Water-Resources Investigations Report 97-4157.
- Lu, J., Wilkinson, M., Haszeldine, R.S., Boyce, A.J., 2010. Carbonate cements in Miller Field of the UK North Sea: a natural analog for mineral trapping in CO₂ geological storage. *Environ. Earth Sci.* 62, 507–517. <http://dx.doi.org/10.1007/s12665-010-0543-1>.
- Mackay, E., Jones, T., Ginty, B., 2012. Oilfield scale management in the Siri asset: paradigm shift due to the use of mixed PWRI/Seawater injection. In: Proceedings of EAGE Annual Conference, Society of Petroleum Engineers (SPE 154534), 4–7 June, 2012. Copenhagen, Denmark.
- Pape, H., Clauser, C., Iffland, J., 2000. Variation of permeability with porosity in sandstone diagenesis interpreted with a fractal pore space model. *Pure Appl. Geophys.* 157, 603–619.
- Parkhurst, D.L., Appelo, C.A.J., 1999. User's guide to PHREEQC (Version 2) – a computer program for speciation, batch-reaction, one-dimensional transport, and inverse geochemical calculations. U.S. Geological Survey, Water-Resources Research Investigation Report 99-425.
- Parkhurst, D.L., Appelo, C.A.J., 2013. Description of input and examples for PHREEQC Version 3 – A computer program for speciation, batch-reaction, one-dimensional transport, and inverse geochemical calculations. U.S. Geological Survey Techniques and Methods, book 6, chapter A43. p. 497. Available only at (<http://pubs.usgs.gov/tm/06/a43>).
- Parkhurst, D.L., Kipp, K.L., Charlton, S.R., 2010. PHAST version 2 – a program for simulating groundwater flow, solute transport, and multicomponent geochemical reactions. U.S. Geological Survey Techniques and Methods 6–A35. p. 235.
- Schlumberger, 2015. Oilfield Glossary. (<http://www.glossary.oilfield.slb.com/en/Terms/s/scale.asp>; accessed on 12.03.2015).
- van Berk, W., Schulz, H.-M., Fu, Y., 2013. Controls on CO₂ fate and behavior in the Gullfaks oilfield (Norway): how hydrogeochemical modeling can help to decipher organic–inorganic interactions. *AAPG Bull.* 97, 253–262. <http://dx.doi.org/10.1111/j.1468-8123.2009.00256.x>.
- Vaughan, P.J., 1987. Analysis of permeability reduction during flow of heated, aqueous fluid through Westerly Granite. In: Tsang, C.F. (Ed.), *Coupled Processes Associated with Nuclear Waste Repositories*. Academic Press, New York, pp. 529–539.
- Verma, A., Pruess, K., 1988. Thermohydrological conditions and silica redistribution near high-level nuclear wastes emplaced in saturated geological formations. *J. Geophys. Res.* 93, 1159–1173.
- Wylde, J.J., Williams, G.D.M., Careil, F., Webb, P., Morris, A., 2005. Deep downhole chemical injection on BP-operated Miller: experience and learning. In: Proceedings of SPE International Symposium on Oilfield Chemistry, Society of Petroleum Engineers (SPE 92832), 2–4 February 2005. Houston, Texas, USA.